

Tracing Power with Circuit Theory

Yu Christine Chen, *Member, IEEE* and Sairaj V. Dhople, *Member, IEEE*

Abstract—Power tracing is the task of disaggregating the power injection of a generator (or a load) into a sum of constituent components that can unambiguously be attributed to loads (generators) and losses. Applications of power tracing range the broad spectrum of: transmission services pricing, loss allocation in distribution networks, fixed-cost allocation, modelling bilateral transactions, and financial storage rights. This paper develops an analytical approach to power tracing leveraging elementary circuit laws. The method is rigorous from a system-theoretic vantage point, and it yields unambiguous results that are consistent with constitutive principles that describe the steady-state behaviour of power networks. Moreover, it can be implemented with limited computational burden, applies to networks with arbitrary topologies, and preserves the coupling between active- and reactive-power injections. Numerical experiments indicate that given a solved power-flow solution, disaggregations can be computed for a test system with 2383 buses, 327 generators, and 2056 loads in 4.34 seconds on a personal computer, hence establishing computational scalability. Furthermore, applications are demonstrated in distribution and transmission networks with case studies focused on quantifying the impact of distributed generation on loss allocation and extracting nodal contributions to bilateral transactions, respectively.

Index Terms—Downstream tracing, Kron reduction, Loss allocation, Power flow, Power tracing, Upstream tracing.

NOMENCLATURE

$\mathcal{G}, \mathcal{L}, \mathcal{N}$	Sets collecting generator, load, and all buses.
$V_{\mathcal{G}}, V_{\mathcal{L}}$	Vectors of voltage phasors at generator and load buses.
$V_{\mathcal{G}}^g, V_{\mathcal{L}}^\ell$	Voltage phasors at generator bus $g \in \mathcal{G}$ and load bus $\ell \in \mathcal{L}$.
$I_{\mathcal{G}}, I_{\mathcal{L}}$	Vectors of current phasors at generator and load buses.
$I_{\mathcal{G}}^g, I_{\mathcal{L}}^\ell$	Current phasors at generator bus $g \in \mathcal{G}$ and load bus $\ell \in \mathcal{L}$.
$S_{\mathcal{G}}, S_{\mathcal{L}}$	Vectors of complex-power injections at generator and load buses.
$S_{\mathcal{G}}^g, S_{\mathcal{L}}^\ell$	Complex-power injections at generator bus $g \in \mathcal{G}$ and load bus $\ell \in \mathcal{L}$.
$Y_{\mathcal{N}}$	Network admittance matrix.
$\gamma_{\mathcal{G}}^\ell, \lambda_{\mathcal{L}}^g$	Portion of the generator g current that is allocated to the load ℓ current and fraction of the load ℓ current sourced from the generator g current.
$\mu_{\mathcal{L}}^g, \delta_{\mathcal{G}}^\ell$	Coefficients capturing portion of generator g complex-power injection that is consumed by load

Y. C. Chen is with the Department of Electrical and Computer Engineering at the University of British Columbia, Vancouver, Canada. E-mail: chen@ECE.UBC.CA. She gratefully acknowledge the support of the Natural Sciences and Engineering Research Council of Canada (NSERC), funding reference number RGPIN-2016-04271.

S. V. Dhople is with the Department of Electrical and Computer Engineering at the University of Minnesota, Minneapolis, MN, USA. E-mail: sdhople@UMN.EDU. He was partially supported by the National Science Foundation (NSF) Sustainability Research Network (SRN) grant-1444745.

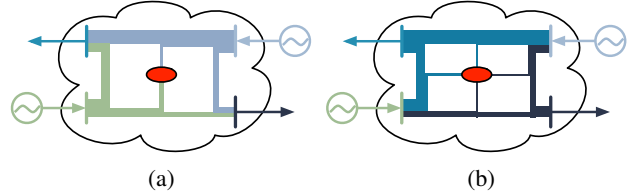


Fig. 1: The proposed tracing approach uncovers (a) downstream and (b) upstream disaggregations that are consistent (fractional components sum up to load and generator values) and unified (allocations include contributions to losses, marked above as red ellipses). Note that the coloured links capture power disaggregations and not the physical topology of the network.

ℓ and portion of load ℓ complex-power injection served by generator g .

L Complex-power loss.

$\omega_{\mathcal{G}}^g, \omega_{\mathcal{L}}^\ell$ Coefficients capturing contributions of generator g and load ℓ to complex-power loss.

I. INTRODUCTION

This paper presents a circuit-theoretic solution to *power tracing*: the problem of disaggregating power injections from a subset of nodes in a power network into a sum of constituent parts that are attributable to other nodes and allocable to losses. It has been hypothesized that an agreeable solution to this problem would pave the way for establishing an optimal regulatory and economic environment for the transparent and efficient operation of power networks [1]–[3]. Furthermore, a universally accepted and analytically justifiable approach to power tracing may potentially also be useful in modelling, analysis, and validation of contemporary notions in power systems economics such as transactive energy [4], peer-to-peer energy trading [5], and blockchain electricity trading [6]. However, as with most modelling and analysis tasks in power networks, nettling nonlinearities pose daunting analytical challenges to power tracing. The majority of previously proposed tracing methods have consequently revolved around numerical approaches, unverifiable assumptions, or sensitivity analysis. Therefore, the merits in a tracing method that is grounded in and conforms to circuit laws that underlie the steady-state behaviour of power networks cannot be overstated.

We consider two types of disaggregations for complex-power injections in the network. In *downstream* tracing, the complex-power injection of a generator is decomposed into a sum of parts that are attributed to loads and losses in the network. Similarly, in *upstream* tracing, the complex power drawn by a load is decomposed into a sum of parts that can be attributed to generators and allocated to the losses. (See Fig. 1 for an illustration.) These are not merely semantic

distinctions, and we demonstrate that they are contextually useful depending on the application at hand. Furthermore, drawing from desirable attributes discussed in [3], we seek a tracing result that is *consistent* and *unified*. A consistent downstream tracing result is one where loads can be demonstrably recovered by summing up fractional decompositions across all generators (and vice versa for the upstream case). A unified disaggregation is one where the decomposition of nodal injections innately embeds allocations to system loss. Namely, losses emerge as integral constituents of the upstream and downstream tracing results, and they are not stitched into the formulations as an afterthought.

Given the fundamental nature of the tracing problem and its latent promise in refashioning power system operations and control tasks, it has attracted extensive attention from several directions. We focus our review of relevant literature squarely on power tracing *methods*, but also reserve a few comments on *applications*. The seminal work in [1] and follow-up efforts in [7]–[10] are grounded in the so-called proportional sharing rule. This is an assumption that at any given bus, outgoing active-power flows on the lines are composed of a sum of parts, which are proportional to the inflows. While these efforts are formative, the proportional sharing method is assumptive by design [8]. Another body of work leverages a variety of graph-theoretic notions to address the tracing problem [2], [11], but these methods lead to iterative computations. Optimization problems with varying degrees of computational complexity offer an appealing numerical alternative [3], [12], [13], but these are inherently algorithmic, and demonstrate tenuous links to the underlying circuit laws that dictate power flows. Previous attempts at leveraging circuit-theoretic notions for power tracing replace constant-power elements with admittance equivalents in an attempt to counter their nonlinearity [14], [15]. While our approach shares this as a common motif, these efforts neither result in *consistent* upstream and downstream disaggregations, nor do they incorporate losses in a *unified* manner. Related efforts that leverage circuit-theoretic notions for the problem of network-usage allocation include [16]–[18]. Finally, we bring attention to literature that has explored applications of power tracing in transmission services pricing [19], loss allocation in distribution networks [20], fixed-cost allocation [3], modelling bilateral transactions [21], [22], and financial storage rights [23].

Unlike most previously proposed approaches that begin with a solved power flow and attempt to *directly* tackle the problem of tracing power, we embark on a more circuitous path, with the intention of ensuring that the method yields consistent and unified results. First, we formulate and propose a solution to the more fundamental problem of tracing currents. Downstream and upstream current tracing can be accomplished with elementary algebraic manipulations of the network admittance matrix while incorporating equivalent-admittance representations of generators and loads. Then, by leveraging fundamental circuit-theoretic definitions, the disaggregation of currents is straightforwardly extended to obtain those of complex-power injections. In this way, the seemingly regressive and obviously unglamorous task of tracing currents emerges as the perfect foil to the more involved problem of tracing power. Since we

deal with complex-valued current and voltage phasors at every step, the resulting upstream and downstream complex-power tracing results preserve the nontrivial couplings between active and reactive powers. For example, our approach quantifies how much of the active power drawn by a particular load derives from both the active- *and* reactive-power injections of generators. To better contextualize the elementary algebraic operations performed on the admittance matrix to arrive at the power tracing results, we establish correspondences with a number of circuit-theoretic notions, including (but not limited to): equivalent admittance representations of nonlinear shunt elements, Kron reduction of complex electrical networks, super-node circuit analysis, and conservation of power.

We summarize salient features of our approach and highlight its contributions over prior art discussed above. First and foremost, the proposed disaggregations of currents (and powers) are grounded in and can be verified to satisfy circuit laws that govern the sinusoidal steady-state behaviour of AC networks. Second, our approach can be applied to both transmission and distribution networks of arbitrary size and topological and constitutional complexity. Given a solved power flow, we trace complex power with minimal computational burden (predominantly attributable to the computation of inverses of admittance and admittance-like matrices). Furthermore, the proposed decompositions preserve and reflect the couplings between active- and reactive-power injections. Finally, the downstream and upstream power-tracing results are consistent and acknowledge losses in a unified manner; these characteristics are conceptually illustrated in Fig. 1.

The remainder of this manuscript is organized as follows. Mathematical notation and the power-system model utilized in the paper are established in Section II. In Section III, we address the downstream disaggregation of generator currents into load contributions (and the corresponding upstream dual). This forms the basis for our main results in Section IV, where we decompose generator power contributions into components that satisfy loads and can be attributed to losses (and the corresponding dual upstream problem). Next, in Section V, we provide two numerical case studies that demonstrate applications of the approach in: i) distribution network loss allocation, and ii) analysis of bilateral transactions in transmission networks. Numerical results from our approach are compared to those generated from the proportional sharing method in [1]. Concluding remarks and directions for future work are offered in Section VI.

II. PRELIMINARIES AND POWER SYSTEM MODEL

Below, we introduce relevant notation and describe the power system model used in the remainder of the paper.

A. Notation

The transpose of a vector or matrix is denoted by $(\cdot)^T$, complex conjugate by $(\cdot)^*$, real and imaginary parts of a complex number by $\text{Re}\{\cdot\}$ and $\text{Im}\{\cdot\}$, respectively, magnitude of a complex scalar by $|\cdot|$, and $j := \sqrt{-1}$. A diagonal matrix formed with entries of the vector X stacked along the main diagonal is denoted by $\text{diag}(X)$. The spaces of N -dimensional

real- and complex-valued vectors are denoted by \mathbb{R}^N and \mathbb{C}^N , respectively; the spaces of $M \times N$ real- and complex-valued matrices are denoted by $\mathbb{R}^{M \times N}$ and $\mathbb{C}^{M \times N}$, respectively. The (m, n) entry, i.e., the entry in the m -th row and n -th column, of the matrix X is denoted by $[X]_{mn}$.

B. Power System Model

Consider an AC network with N buses, collected in the set \mathcal{N} , operating in sinusoidal steady state. We partition the N buses in the network into G generator buses collected in the set $\mathcal{G} = \{1, \dots, G\} \subseteq \mathcal{N}$; and L load buses collected in the set $\mathcal{L} = \mathcal{N} \setminus \mathcal{G} = \{G+1, \dots, N\}$. Aligned with standard practices in steady-state power-system modelling, we adopt constant power load (CPL) models which imply that at these buses, a fixed amount of active and reactive power is drawn. On the other hand, generators are modelled as constant power sources (CPSs). This is reasonable, since we assume that a solved power flow is available, and consequently, both the active- and reactive-power injections can be computed for the generators. The set of transmission lines is represented by $\mathcal{E} := \{(m, n)\} \subseteq \mathcal{N} \times \mathcal{N}$. Each line is modelled using the Π -model with series admittance $y_{mn} = g_{mn} + jb_{mn} \in \mathbb{C}$ and shunt admittance $y_{mn}^{\text{sh}} \in \mathbb{C}$. Denote the vector of shunt admittances by $Y_{\text{sh}} = [y_1, \dots, y_N]^T \in \mathbb{C}^N$, where

$$y_m := y_{mm} + \sum_{k \in \mathcal{N}_m} y_{mk}^{\text{sh}} = g_m + jb_m \quad (1)$$

is the total shunt admittance connected to bus m , $\mathcal{N}_m \subseteq \mathcal{N}$ denotes the set of neighbours of bus m , and $y_{mm} \in \mathbb{C}$ captures passive shunt elements connected to bus m . With the above model in place, the network admittance matrix, denoted by $Y_{\mathcal{N}}$, can be expressed as

$$Y_{\mathcal{N}} = Y + \text{diag}(Y_{\text{sh}}), \quad (2)$$

where entries of Y are given by

$$[Y]_{mn} := \begin{cases} \sum_{(m,k) \in \mathcal{E}} y_{mk}, & \text{if } m = n, \\ -y_{mn}, & \text{if } (m, n) \in \mathcal{E}, \\ 0, & \text{otherwise.} \end{cases} \quad (3)$$

Nodal voltages of generators and loads are denoted by

$$\begin{aligned} V_{\mathcal{G}} &= [V_1, \dots, V_G]^T =: [V_{\mathcal{G}}^1, \dots, V_{\mathcal{G}}^G]^T \in \mathbb{C}^G, \\ V_{\mathcal{L}} &= [V_{G+1}, \dots, V_N]^T =: [V_{\mathcal{L}}^{G+1}, \dots, V_{\mathcal{L}}^N]^T \in \mathbb{C}^L, \end{aligned} \quad (4)$$

respectively, where $V_i = |V_i| \angle \theta_i \in \mathbb{C}$ represents the voltage phasor at bus i . Also, denote the vectors of current injections into generator and load buses by

$$\begin{aligned} I_{\mathcal{G}} &= [I_1, \dots, I_G]^T =: [I_{\mathcal{G}}^1, \dots, I_{\mathcal{G}}^G]^T \in \mathbb{C}^G, \\ I_{\mathcal{L}} &= [I_{G+1}, \dots, I_N]^T =: [I_{\mathcal{L}}^{G+1}, \dots, I_{\mathcal{L}}^N]^T \in \mathbb{C}^L, \end{aligned} \quad (5)$$

respectively, where $I_i \in \mathbb{C}$ denotes the phasor of the net current injected into bus i from the ground node. This includes the current through any shunt elements connected to bus i ; see Fig. 2 for an illustration. Kirchhoff's current law (KCL) applied at all buses can be compactly represented in matrix-vector form as

$$\begin{bmatrix} I_{\mathcal{G}} \\ I_{\mathcal{L}} \end{bmatrix} = \begin{bmatrix} Y_{\mathcal{G}\mathcal{G}} & Y_{\mathcal{G}\mathcal{L}} \\ Y_{\mathcal{L}\mathcal{G}}^T & Y_{\mathcal{L}\mathcal{L}} \end{bmatrix} \begin{bmatrix} V_{\mathcal{G}} \\ V_{\mathcal{L}} \end{bmatrix}, \quad (6)$$

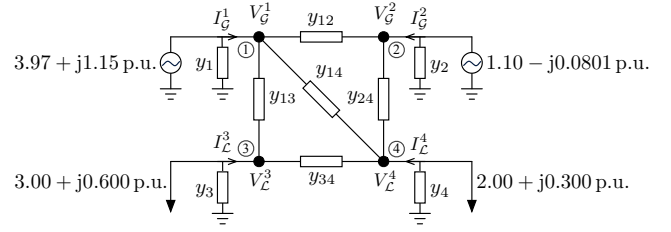


Fig. 2: One-line diagram for a 4-bus network illustrating adopted notation. The network is composed of generators at buses in $\mathcal{G} = \{1, 2\}$ and loads at buses in $\mathcal{L} = \{3, 4\}$.

TABLE I: Power-flow solution for 4-bus system in Fig. 2. All quantities are in p.u.

Bus Voltages		Current Injections		Power Injections	
$V_{\mathcal{G}}^1$	$1.04 \angle 0^\circ$	$I_{\mathcal{G}}^1$	$3.81 - j1.32$	$S_{\mathcal{G}}^1$	$3.97 + j1.37$
$V_{\mathcal{G}}^2$	$1.02 \angle -2.61^\circ$	$I_{\mathcal{G}}^2$	$1.07 - j0.104$	$S_{\mathcal{G}}^2$	$1.10 + j0.0562$
$V_{\mathcal{L}}^3$	$0.978 \angle -12.4^\circ$	$I_{\mathcal{L}}^3$	$-2.91 + j1.03$	$S_{\mathcal{L}}^3$	$-3.00 - j0.379$
$V_{\mathcal{L}}^4$	$0.994 \angle -8.88^\circ$	$I_{\mathcal{L}}^4$	$-1.98 + j0.385$	$S_{\mathcal{L}}^4$	$-2.00 - j0.0746$

where $Y_{\mathcal{G}\mathcal{G}} \in \mathbb{C}^{G \times G}$, $Y_{\mathcal{G}\mathcal{L}} \in \mathbb{C}^{G \times L}$, and $Y_{\mathcal{L}\mathcal{L}} \in \mathbb{C}^{L \times L}$ are (dimensionally consistent) decompositions of the admittance matrix Y . Finally, mirroring the notation adopted in (4)–(5), the nodal complex-power injections into the generator bus $g \in \mathcal{G}$ and load bus $\ell \in \mathcal{L}$ are expressed as

$$S_{\mathcal{G}}^g = V_{\mathcal{G}}^g (I_{\mathcal{G}}^g)^*, \quad S_{\mathcal{L}}^\ell = V_{\mathcal{L}}^\ell (I_{\mathcal{L}}^\ell)^*. \quad (7)$$

The complex-power injections above are decomposed into real and imaginary parts as follows: $S_{\mathcal{G}}^g = P_{\mathcal{G}}^g + jQ_{\mathcal{G}}^g$ and $S_{\mathcal{L}}^\ell = P_{\mathcal{L}}^\ell + jQ_{\mathcal{L}}^\ell$.

The notation introduced so far is illustrated with a simple example next. We will periodically revisit this example in the paper to demonstrate key concepts numerically.

Example 1. Consider the 4-bus system with the one-line diagram shown in Fig. 2. Generators are connected at buses in the set $\mathcal{G} = \{1, 2\}$, and loads at buses in the set $\mathcal{L} = \{3, 4\}$. Voltage magnitudes at buses 1 and 2 are regulated to be $|V_{\mathcal{G}}^1| = 1.04$ p.u. and $|V_{\mathcal{G}}^2| = 1.02$ p.u., respectively. Transmission lines are modelled with lumped parameters, with $y_{12} = 0.553 - j10.5$, $y_{12}^{\text{sh}} = j0.0880$, $y_{13} = 0.771 - j10.5$, $y_{13}^{\text{sh}} = j0.0790$, $y_{14} = -j6.90$, $y_{14}^{\text{sh}} = j0.0330$, $y_{24} = 2.00 - j14.0$, $y_{24}^{\text{sh}} = j0.0430$, $y_{34} = -j11.8$, and $y_{34}^{\text{sh}} = j0.152$, all in p.u. The power-flow solution is reported in Table I (computed with bus 1 set to be the slack bus). ■

III. TRACING CURRENTS

In this section, we address the problem of decomposing a particular generator current injection into constituent parts that identifiably serve loads, as well as the dual problem of extracting generator contributions that serve a particular load. To begin, we establish some terminology:

- 1) *Downstream current tracing:* Currents injected by generators are disaggregated into components that are attributed to loads. Specifically, we decompose the current injected by the g generator, $I_{\mathcal{G}}^g$, as a linear combination of entries of $I_{\mathcal{L}}$ as follows:

$$I_{\mathcal{G}}^g = \sum_{\ell \in \mathcal{L}} \gamma_g^\ell I_{\mathcal{L}}^\ell, \quad \forall g \in \mathcal{G}. \quad (8)$$

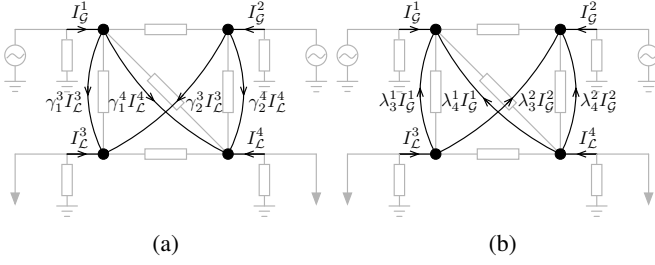


Fig. 3: (a) Downstream and (b) upstream current tracing for the 4-bus network in Fig. 2. Our approach uncovers the coefficients $(\gamma_1^3, \gamma_1^4, \gamma_2^3, \gamma_2^4)$ and $(\lambda_1^3, \lambda_1^4, \lambda_2^3, \lambda_2^4)$ in closed form. We demonstrate that $\gamma_1^3 + \gamma_2^3 = -1$, $\gamma_1^4 + \gamma_2^4 = -1$; and $\lambda_3^1 + \lambda_4^1 = -1$, $\lambda_3^2 + \lambda_4^2 = -1$. (Only grey-coloured edges correspond to physical interconnections.)

For the 4-bus system in Fig. 2, the notion of downstream current tracing in (8) is illustrated in Fig. 3a.

- 2) *Upstream current tracing*: Currents injected by loads are disaggregated into components that are identifiably sourced from generators. Specifically, we decompose the current injected by the ℓ load, $I_{\mathcal{L}}^{\ell}$, as a linear combination of entries of $I_{\mathcal{G}}$ as follows:

$$I_{\mathcal{L}}^{\ell} = \sum_{g \in \mathcal{G}} \lambda_g^{\ell} I_{\mathcal{G}}^g, \quad \forall \ell \in \mathcal{L}. \quad (9)$$

For the 4-bus system in Fig. 2, the notion of upstream current tracing in (9) is illustrated in Fig. 3b.

The coefficients γ_g^{ℓ} and λ_g^{ℓ} in (8) and (9) can be determined $\forall g \in \mathcal{G}, \ell \in \mathcal{L}$ given the topology of the network and the solved power flow. We discuss this next.

A. Downstream Current Tracing

In this section, we derive the coefficients γ_g^{ℓ} in analytical closed form. We present this in the form of a lemma next, following which, several remarks are provided to explain the result from a circuit-theoretic perspective.

Lemma 1 (Downstream Current Tracing). The current injected by generator $g \in \mathcal{G}$, $I_{\mathcal{G}}^g$, can be uniquely disaggregated into a linear combination of currents injected into each load bus, as follows:

$$I_{\mathcal{G}}^g = \sum_{\ell \in \mathcal{L}} \gamma_g^{\ell} I_{\mathcal{L}}^{\ell}, \quad \forall g \in \mathcal{G}. \quad (10)$$

In (10), $\gamma_g^{\ell} \in \mathbb{C}$ is the (g, ℓ) entry of the $G \times L$ matrix

$$\Gamma = (Y_{\mathcal{G}\mathcal{L}} - Y_{\mathcal{G}\mathcal{G}}(Y_{\mathcal{G}\mathcal{G}} - \text{diag}(\Upsilon_{\mathcal{G}}))^{-1}Y_{\mathcal{G}\mathcal{L}})Y_{\mathcal{L}}^{-1}, \quad (11)$$

where $Y_{\mathcal{L}} \in \mathbb{C}^{L \times L}$ is given by

$$Y_{\mathcal{L}} = Y_{\mathcal{L}\mathcal{L}} - Y_{\mathcal{G}\mathcal{L}}^T(Y_{\mathcal{G}\mathcal{G}} - \text{diag}(\Upsilon_{\mathcal{G}}))^{-1}Y_{\mathcal{G}\mathcal{L}}, \quad (12)$$

and $\Upsilon_{\mathcal{G}} \in \mathbb{C}^G$ satisfies the following relationship, which captures the power-flow solution at the G generator buses:

$$I_{\mathcal{G}} = \text{diag}(\Upsilon_{\mathcal{G}})V_{\mathcal{G}}. \quad (13)$$

Proof. Substituting (13) into (6) yields

$$\begin{bmatrix} 0_{\mathcal{G}} \\ I_{\mathcal{L}} \end{bmatrix} = \begin{bmatrix} Y_{\mathcal{G}\mathcal{G}} - \text{diag}(\Upsilon_{\mathcal{G}}) & Y_{\mathcal{G}\mathcal{L}} \\ Y_{\mathcal{G}\mathcal{L}}^T & Y_{\mathcal{L}\mathcal{L}} \end{bmatrix} \begin{bmatrix} V_{\mathcal{G}} \\ V_{\mathcal{L}} \end{bmatrix}, \quad (14)$$

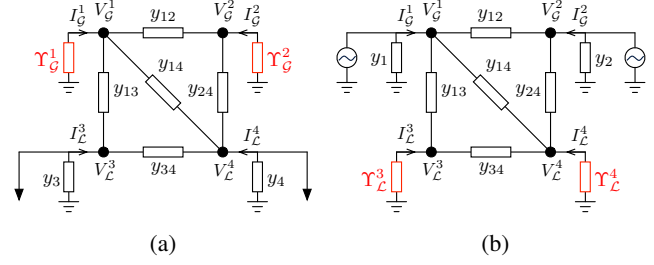


Fig. 4: Equivalent-admittance models for generators and loads, highlighted in red, are used in (a) downstream, and (b) upstream tracing, for the network in Fig. 2.

where $0_{\mathcal{G}}$ is a G -length vector of all zeros. Elementary algebraic manipulations of (14) yield the following expressions:

$$\begin{aligned} I_{\mathcal{L}} &= (Y_{\mathcal{L}\mathcal{L}} - Y_{\mathcal{G}\mathcal{L}}^T(Y_{\mathcal{G}\mathcal{G}} - \text{diag}(\Upsilon_{\mathcal{G}}))^{-1}Y_{\mathcal{G}\mathcal{L}})V_{\mathcal{L}} =: Y_{\mathcal{L}}V_{\mathcal{L}}, \\ V_{\mathcal{G}} &= -(Y_{\mathcal{G}\mathcal{G}} - \text{diag}(\Upsilon_{\mathcal{G}}))^{-1}Y_{\mathcal{G}\mathcal{L}}V_{\mathcal{L}}. \end{aligned} \quad (15)$$

Isolating $I_{\mathcal{G}}$ from (6), we get

$$I_{\mathcal{G}} = Y_{\mathcal{G}\mathcal{G}}V_{\mathcal{G}} + Y_{\mathcal{G}\mathcal{L}}V_{\mathcal{L}}. \quad (16)$$

Substituting $V_{\mathcal{G}} = -(Y_{\mathcal{G}\mathcal{G}} - \text{diag}(\Upsilon_{\mathcal{G}}))^{-1}Y_{\mathcal{G}\mathcal{L}}V_{\mathcal{L}}$ and $V_{\mathcal{L}} = Y_{\mathcal{L}}^{-1}I_{\mathcal{L}}$ from (15) into (16), we get

$$\begin{aligned} I_{\mathcal{G}} &= (Y_{\mathcal{G}\mathcal{L}} - Y_{\mathcal{G}\mathcal{G}}(Y_{\mathcal{G}\mathcal{G}} - \text{diag}(\Upsilon_{\mathcal{G}}))^{-1}Y_{\mathcal{G}\mathcal{L}})Y_{\mathcal{L}}^{-1}I_{\mathcal{L}} \\ &=: \Gamma I_{\mathcal{L}}. \end{aligned} \quad (17)$$

Extracting the g -th entry of $I_{\mathcal{G}}$ in (17), we arrive at (10). ■

1) *Circuit-theoretic Interpretation*: We provide a few remarks that yield a circuit-theoretic interpretation to two key terms in Lemma 1: the vector $\Upsilon_{\mathcal{G}}$ and the matrix $Y_{\mathcal{L}}$. First, with regard to $\Upsilon_{\mathcal{G}}$, note that the disaggregation in (10) would be algebraically consistent with any complex-valued $G \times G$ matrix, say Υ , which can satisfy the power-flow solution $I_{\mathcal{G}} = \Upsilon V_{\mathcal{G}}$. However, *only* a diagonal matrix: i) can be uniquely determined given $I_{\mathcal{G}}$ and $V_{\mathcal{G}}$, and ii) preserves the topology of the network. This establishes the uniqueness of the disaggregation, and lends an appealing circuit-theoretic interpretation to the entries of $\Upsilon_{\mathcal{G}}$. Particularly, given the steady-state power-flow solution in (7), entries of the vector $\Upsilon_{\mathcal{G}}$ are (almost surely not realizable) equivalent-admittance representations of the generators. As an example, with $\Upsilon_{\mathcal{G}}^1 = I_{\mathcal{G}}^1/V_{\mathcal{G}}^1$ and $\Upsilon_{\mathcal{G}}^2 = I_{\mathcal{G}}^2/V_{\mathcal{G}}^2$, the circuit in Fig. 4a is equivalent to the one in Fig. 2 in sinusoidal steady state. With regard to $Y_{\mathcal{L}}$, note that it corresponds to the admittance matrix of the Kron-reduced network where all generator buses (modelled with admittances $\Upsilon_{\mathcal{G}}$) are eliminated. As an example, the network in Fig. 4a reduces to the one in Fig. 5a through this process.

2) *Consistency*: Notice that γ_g^{ℓ} precisely represents the fractional contribution of the load ℓ current to the generator g current. Indeed, the values of γ_g^{ℓ} are such that

$$\sum_{g \in \mathcal{G}} \gamma_g^{\ell} = -1, \quad \forall \ell \in \mathcal{L}, \quad (18)$$

which implies that we can express $I_{\mathcal{L}}^{\ell} = -\sum_{g \in \mathcal{G}} \gamma_g^{\ell} I_{\mathcal{G}}^g$. This conclusively establishes the consistency of the disaggregation in (10), since it implies that the ℓ -th load current can be

TABLE II: Current tracing for 4-bus system in Fig. 2. All quantities are in p.u.

(a) Downstream			(b) Upstream				
	$\gamma_1^3 I_{\mathcal{L}}^3$	$\gamma_2^4 I_{\mathcal{L}}^4$	Row Σ	$\lambda_1^1 I_{\mathcal{G}}^1$	$\lambda_2^2 I_{\mathcal{G}}^2$	Row Σ	
$I_{\mathcal{G}}^1$	2.26-j0.948	1.55-j0.368	3.81-j1.32	$I_{\mathcal{L}}^3$	-2.27+j0.918	-0.644+j0.116	-2.91+j1.03
$I_{\mathcal{G}}^2$	0.652-j0.0868	0.423-j0.0172	1.07-j0.104	$I_{\mathcal{L}}^4$	-1.55+j0.397	-0.431-j0.0122	-1.98+j0.385
Column Σ	2.91-j1.03	1.98-j0.385	4.89-j1.42	Column Σ	-3.81+j1.32	-1.07+j0.104	-4.89+j1.42
	$-I_{\mathcal{L}}^3$	$-I_{\mathcal{L}}^4$	$\sum_{g \in \mathcal{G}} I_{\mathcal{G}}^g$		$-I_{\mathcal{G}}^1$	$-I_{\mathcal{G}}^2$	$\sum_{\ell \in \mathcal{L}} I_{\mathcal{L}}^{\ell}$

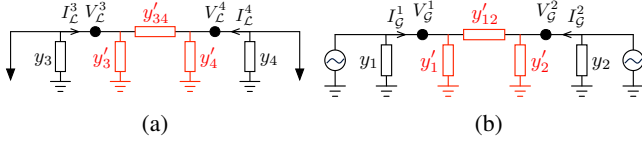


Fig. 5: Kron-reduced networks from Fig. 4 are highlighted in red. (a) From Fig. 4a with admittance matrix $Y_{\mathcal{L}}$, i.e., $I_{\mathcal{L}} = Y_{\mathcal{L}} V_{\mathcal{L}}$. (b) From Fig. 4b with admittance matrix $Y_{\mathcal{G}}$, i.e., $I_{\mathcal{G}} = Y_{\mathcal{G}} V_{\mathcal{G}}$.

recovered by summing up its contributions to all generators in the system. The identity in (18) can be proved as follows. Sum up both sides of (10) over all generators to get

$$\sum_{g \in \mathcal{G}} I_{\mathcal{G}}^g = \sum_{g \in \mathcal{G}} \sum_{\ell \in \mathcal{L}} \gamma_g^{\ell} I_{\mathcal{L}}^{\ell} = \sum_{\ell \in \mathcal{L}} \sum_{g \in \mathcal{G}} \gamma_g^{\ell} I_{\mathcal{L}}^{\ell}, \quad (19)$$

where the second equality above follows by simply switching the order of summation. Also, treating the network as a supernode, we get from KCL that

$$\sum_{g \in \mathcal{G}} I_{\mathcal{G}}^g = - \sum_{\ell \in \mathcal{L}} I_{\mathcal{L}}^{\ell}. \quad (20)$$

Since (19) and (20) hold $\forall I_{\mathcal{L}}, I_{\mathcal{G}}$, we see that (18) is true.

Example 2. Here, we illustrate the downstream current-tracing ideas introduced above using the 4-bus system described in Example 1. See Fig. 3a for an illustration. In Table II–(a), given the steady-state power-flow solution, we compute the disaggregation of generator current injections into load contributions as described in (10). We note that the rows expectedly sum to generator current injections, indicating the validity of the decomposition. It is also consistent, because in Table II–(a), columns 2 and 3 sum up as follows: $\gamma_1^3 I_{\mathcal{L}}^3 + \gamma_2^3 I_{\mathcal{L}}^3 = -I_{\mathcal{L}}^3$ and $\gamma_1^4 I_{\mathcal{L}}^4 + \gamma_2^4 I_{\mathcal{L}}^4 = -I_{\mathcal{L}}^4$. Thus, as indicated in (18), it is indeed the case that $\gamma_1^3 + \gamma_2^3 = -1$ and $\gamma_1^4 + \gamma_2^4 = -1$. ■

B. Upstream Current Tracing

Next, mirroring the result in Lemma 1, we derive in closed form the coefficients λ_{ℓ}^g that allow the disaggregation of load currents into contributions from generators.

Corollary 1 (Upstream Current Tracing). The current injected by load $\ell \in \mathcal{L}$, $I_{\mathcal{L}}^{\ell}$, can be uniquely disaggregated into a linear combination of currents injected into each generator bus,

$$I_{\mathcal{L}}^{\ell} = \sum_{g \in \mathcal{G}} \lambda_{\ell}^g I_{\mathcal{G}}^g. \quad (21)$$

In (21), $\lambda_{\ell}^g \in \mathbb{C}$ is the (ℓ, g) entry of the $L \times G$ matrix

$$\Lambda = (Y_{\mathcal{G}}^{\text{T}} - Y_{\mathcal{L}\mathcal{L}}(Y_{\mathcal{L}\mathcal{L}} - \text{diag}(\Upsilon_{\mathcal{L}}))^{-1} Y_{\mathcal{G}\mathcal{L}}^{\text{T}}) Y_{\mathcal{G}}^{-1}, \quad (22)$$

where $Y_{\mathcal{G}} \in \mathbb{C}^{G \times G}$ is given by

$$Y_{\mathcal{G}} = Y_{\mathcal{G}\mathcal{G}} - Y_{\mathcal{G}\mathcal{L}}(Y_{\mathcal{L}\mathcal{L}} - \text{diag}(\Upsilon_{\mathcal{L}}))^{-1} Y_{\mathcal{G}\mathcal{L}}^{\text{T}}, \quad (23)$$

and $\Upsilon_{\mathcal{L}} \in \mathbb{C}^L$ satisfies the following relationship, which captures the power-flow solution at the L load buses:

$$I_{\mathcal{L}} = \text{diag}(\Upsilon_{\mathcal{L}}) V_{\mathcal{L}}. \quad (24)$$

Proof. The result above can be derived in an analogous fashion to Lemma 1 and the derivation is not included. ■

Offering due respect to brevity, we refrain from repeating detailed remarks on the circuit-theoretic interpretation to entries of $\Upsilon_{\mathcal{L}}$, and the fact that $Y_{\mathcal{G}}$ represents the Kron-reduced admittance matrix of the network where all load buses (modelled with admittances $\Upsilon_{\mathcal{L}}$) are eliminated. As an illustration of these ideas for the upstream tracing case, equivalent-admittance models for the CPLs in Fig. 2 are computed to give rise to the circuit in Fig. 4b, which reduces to the one in Fig. 5b through Kron reduction of all load buses (modelled with admittances $\Upsilon_{\mathcal{L}}$). Furthermore, in this case,

$$\sum_{\ell \in \mathcal{L}} \lambda_{\ell}^g = -1, \quad \forall g \in \mathcal{G}. \quad (25)$$

This implies that we can express $I_{\mathcal{G}}^g = - \sum_{\ell \in \mathcal{L}} \lambda_{\ell}^g I_{\mathcal{L}}^{\ell}$, which establishes the consistency of the disaggregation in (21).

Example 3. Revisiting the 4-bus system from Example 1, we illustrate the upstream current-tracing concepts introduced above. See Fig. 3b for an illustration. Table II–(b) reports pertinent quantities obtained by disaggregating load-current injections into generator contributions following (21). We first observe that the decomposition is valid as the rows sum to load current injections. Also, consistency is demonstrated by the fact that $\lambda_3^1 + \lambda_4^1 = -1$ and $\lambda_3^2 + \lambda_4^2 = -1$, as indicated in columns 2 and 3 of Table II–(b), which show $\lambda_3^1 I_{\mathcal{L}}^3 + \lambda_4^1 I_{\mathcal{L}}^3 = -I_{\mathcal{L}}^3$ and $\lambda_3^2 I_{\mathcal{L}}^4 + \lambda_4^2 I_{\mathcal{L}}^4 = -I_{\mathcal{L}}^4$. ■

IV. TRACING COMPLEX POWER

In this section, we address the problem of disaggregating the generator complex-power outputs into contributions to the loads and system losses (and the dual problem). To aid the discussion, we define—while mildly abusing terminology and notation¹—the complex-power loss in the system as

$$L = \sum_{g \in \mathcal{G}} S_{\mathcal{G}}^g + \sum_{\ell \in \mathcal{L}} S_{\mathcal{L}}^{\ell}. \quad (26)$$

System loss is typically defined as the real part of (26), which includes line losses [24]. We generalize this definition

¹The variable L was previously used to denote the number of load buses. Subsequent usage, however, should be contextually obvious.

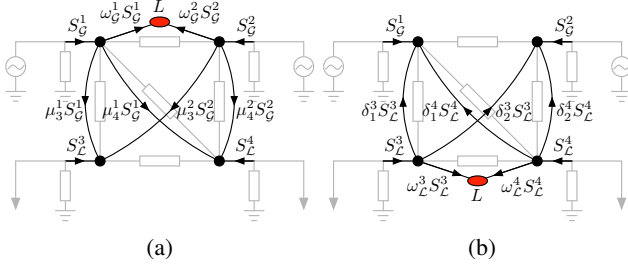


Fig. 6: (a) Downstream and (b) upstream complex-power tracing in the 4-bus network. Our approach uncovers in closed form the coefficients $(\mu_3^1, \mu_4^1, \mu_3^2, \mu_4^2)$ and $(\delta_3^3, \delta_4^3, \delta_3^4, \delta_4^4)$, as well as (ω_G^1, ω_G^2) and (ω_L^3, ω_L^4) . Coefficients (ω_G^1, ω_G^2) and (ω_L^3, ω_L^4) enable allocation of complex-power loss, L (marked as a red ellipse), to generator and load complex-power injections, respectively. (Only grey-coloured edges correspond to physical interconnections.)

to its complex-valued counterpart to ensure consistency in subsequent developments, where we uncover contributions of generator and load buses to system loss. As such, the resulting disaggregations in downstream and upstream tracing naturally incorporate allocations of line losses to the generators and loads in the network, respectively.

With the definition of system loss in place, we now introduce notions of downstream and upstream tracing:

- 1) *Downstream power tracing*: The complex-power output of generators are disaggregated into contributions to system losses and components that are consumed by the loads in the network. For the 4-bus system in Fig. 2, the notion of downstream tracing is illustrated in Fig. 6a.
- 2) *Upstream power tracing*: The complex power consumed by each load is disaggregated into its contribution to system losses and components that are identifiably sourced from generators. For the 4-bus system in Fig. 2, the notion of upstream tracing is illustrated in Fig. 6b.

Both downstream and upstream complex-power tracing draw from and build upon the current tracing results in Section III.

A. Downstream Power Tracing

Here, we state one of the main results of this paper, which pertains to the decomposition of generator complex-power injections into constituent parts that are: i) consumed by each load in the network, and ii) allocated to system loss.

Theorem 1 (Downstream Power Tracing). Express the complex-power injection at generator bus g as follows:

$$S_G^g = \omega_G^g S_G^g + \sum_{\ell \in \mathcal{L}} \mu_\ell^g S_G^g. \quad (27)$$

With the choice

$$\mu_\ell^g = -\frac{V_\ell^\ell}{V_G^g} (\lambda_\ell^g)^*, \quad \omega_G^g = 1 - \sum_{\ell \in \mathcal{L}} \mu_\ell^g, \quad (28)$$

where V_ℓ^ℓ and V_G^g denote the nodal voltages of the ℓ load and g generator buses, respectively, and $\lambda_\ell^g = [\Lambda]_{\ell g}$ (see (22)), we have the following:

- (1) The fractional component of generator g output that is consumed by load ℓ is given by $\mu_\ell^g S_G^g$, i.e.,

$$S_\ell^\ell = -\sum_{g \in \mathcal{G}} \mu_\ell^g S_G^g, \quad \forall \ell \in \mathcal{L}. \quad (29)$$

- (2) The contribution of generator g to the complex-power loss, L , is given by $\omega_G^g S_G^g$, i.e.,

$$L = \sum_{g \in \mathcal{G}} \omega_G^g S_G^g. \quad (30)$$

Before delving into the proof to (29) and (30), a few remarks are in order. The decomposition of S_G^g into the terms $\omega_G^g S_G^g$ and $\{\mu_\ell^g S_G^g\}_{\ell \in \mathcal{L}}$ is *not* profound. Particularly, for any set of complex variables, $\{\mu_\ell^g\}_{\ell \in \mathcal{L}}$, and with the choice $\omega_G^g = 1 - \sum_{\ell \in \mathcal{L}} \mu_\ell^g$, the expression in (27) is algebraically consistent, i.e., the right hand side sums to S_G^g . What is to be emphasized is that with the particular choice of μ_ℓ^g in (28), the terms $\mu_\ell^g S_G^g$ and $\omega_G^g S_G^g$ represent the contribution of the g -th generator output to the ℓ -th load and to the system losses, respectively. This is established in (29) and (30), which we prove next.

Proof. To show (29), express the complex-power injection into load bus $\ell \in \mathcal{L}$ as follows:

$$S_\ell^\ell = V_\ell^\ell (I_\ell^\ell)^*. \quad (31)$$

Substitute for I_ℓ^ℓ from (21) into the above to get

$$\begin{aligned} S_\ell^\ell &= V_\ell^\ell \left(\sum_{g \in \mathcal{G}} \lambda_\ell^g I_G^g \right)^* = \sum_{g \in \mathcal{G}} V_\ell^\ell (\lambda_\ell^g I_G^g)^* \\ &= \sum_{g \in \mathcal{G}} \frac{V_\ell^\ell}{V_G^g} (\lambda_\ell^g)^* S_G^g =: -\sum_{g \in \mathcal{G}} \mu_\ell^g S_G^g, \end{aligned} \quad (32)$$

where the third equality above is obtained by substituting $(I_G^g)^* = S_G^g / V_G^g$.

Next, to show (30), substitute for S_ℓ^ℓ from (29) into (26) and consider the following steps:

$$\begin{aligned} L &= \sum_{g \in \mathcal{G}} S_G^g - \sum_{\ell \in \mathcal{L}} \sum_{g \in \mathcal{G}} \mu_\ell^g S_G^g = \sum_{g \in \mathcal{G}} S_G^g - \sum_{g \in \mathcal{G}} \sum_{\ell \in \mathcal{L}} \mu_\ell^g S_G^g \\ &= \sum_{g \in \mathcal{G}} \left(1 - \sum_{\ell \in \mathcal{L}} \mu_\ell^g \right) S_G^g =: \sum_{g \in \mathcal{G}} \omega_G^g S_G^g. \end{aligned} \quad (33)$$

This completes the proof. \blacksquare

B. Upstream Power Tracing

Mirroring the result in Theorem 1, below, we address the problem of disaggregating the complex-power consumed by loads into constituent parts that are: i) identifiably sourced from each generator, and ii) allocated to system loss.

Corollary 2 (Upstream Power Tracing). Express the complex-power injection of load bus ℓ as follows:

$$S_\ell^\ell = \omega_L^\ell S_\ell^\ell + \sum_{g \in \mathcal{G}} \delta_g^\ell S_\ell^\ell. \quad (34)$$

With the choice

$$\delta_g^\ell = -\frac{V_G^g}{V_\ell^\ell} (\gamma_g^\ell)^*, \quad \omega_L^\ell = 1 - \sum_{g \in \mathcal{G}} \delta_g^\ell, \quad (35)$$

TABLE III: Complex-power tracing for 4-bus system in Fig. 2. All quantities are in p.u.

(a) Downstream				(b) Upstream					
	$\mu_3^g S_G^g$	$\mu_4^g S_G^g$	$\omega_g^g S_G^g$	Row Σ		$\delta_1^\ell S_L^\ell$	$\delta_2^\ell S_L^\ell$	$\omega_L^\ell S_L^\ell$	Row Σ
S_L^1	2.36+j0.403	1.58+j0.153	0.0274+j0.813	3.97+j1.37	S_L^3	-2.35-j0.986	-0.668-j0.0582	0.0194+j0.665	-3.00-j0.379
S_G^2	0.640-j0.0237	0.421-j0.0781	0.0389+j0.158	1.10+j0.0562	S_L^4	-1.62-j0.382	-0.432+j0.0021	0.0469+j0.306	-2.00-j0.0746
Column Σ	3.00+j0.379	2.00-j0.0746	0.0664+j0.970	5.07+j1.42	Column Σ	-3.97-j1.37	-1.10-j0.0562	0.0664+j0.970	-5.00-j0.454
	$-S_L^3$	$-S_L^4$	L	$\sum_{g \in \mathcal{G}} S_G^g$		$-S_G^3$	$-S_G^4$	L	$\sum_{\ell \in \mathcal{L}} S_L^\ell$

TABLE IV: Comparison of (a) downstream and (b) upstream tracing results for 4-bus system in Example 1 obtained via the proposed method and the one in [1]. All quantities are in p.u.

[Proposed]				[1]				
	Bus	(3)	(4)	Loss	Bus	(3)	(4)	Loss
(a) Downstream	(1)	2.36	1.58	0.0274	(1)	2.72	1.20	0.0489
	(2)	0.640	0.421	0.0389	(2)	0.279	0.804	0.0174
(b) Upstream	Bus	(1)	(2)	Loss	Bus	(1)	(2)	Loss
	(3)	-2.35	-0.668	0.0194	(3)	-2.76	-0.382	0.0463
	(4)	-1.62	-0.432	0.0469	(4)	-1.20	-0.817	0.0201

where V_L^ℓ and V_G^g denote the nodal voltages of the ℓ load and g generator buses, respectively, and $\gamma_g^\ell = [\Gamma]_{g\ell}$ (see (11)), we have the following:

- (1) The fractional component of load ℓ that is served by generator g is given by $\delta_g^\ell S_L^\ell$, i.e.,

$$S_G^g = - \sum_{\ell \in \mathcal{L}} \delta_g^\ell S_L^\ell, \quad \forall g \in \mathcal{G}. \quad (36)$$

- (2) The contribution of load ℓ to the complex-power loss, L , is given by $\omega_L^\ell S_L^\ell$, i.e.,

$$L = \sum_{\ell \in \mathcal{L}} \omega_L^\ell S_L^\ell. \quad (37)$$

Proof. The proof proceeds analogously to that for Theorem 1 and is omitted in the interest of brevity. ■

The power-tracing results highlighted in (27) and (34) are consistent and unified. In particular, notice that (29) establishes consistency in downstream tracing since the fractional decompositions across all generators *demonstrably* sum up to loads. Analogously, (36) establishes consistency in upstream tracing. Furthermore, notice from (30) and (37) that the results are unified since the compositional decomposition of generators and loads *innately* include allocations to system loss.

Example 4. Direct application of (27) to the 4-bus system from Example 1 yields disaggregation of generator complex-power injections, pertinent values from which are reported in Table III–(a). For instance, the complex-power injection at bus 1 is $3.97 + j1.37$ p.u., out of which $2.36 + 0.403$ p.u. is consumed by the load at bus 3, $1.58 + 0.153$ p.u. is consumed by the load at bus 4, and $0.0274 + 0.813$ p.u. is—for lack of a better word—*dissipated* as loss. The contributions to loss from the two generators sum to $0.0664 + j0.970$ p.u., which indeed coincides with the total system loss as defined in (26) and computed using the power-flow solution in Table I. See Fig. 6a for an illustration.

On the other hand, the disaggregation of load complex-power injections in the 4-bus system from Example 1 is obtained by applying (34) and is reported in Table III–(b). See Fig. 6b for an illustration. As an example, the load at

bus 3 sources $2.35 + j0.986$ p.u. from the generator at bus 1 and $0.668 + j0.0582$ p.u. from the generator at bus 2, out of which $3.00 + j0.379$ p.u. is consumed by the load itself while $0.0194 + j0.665$ p.u. is allocated to system loss.

For comparison, in Table IV, we report results obtained using the active-power tracing method in [1]. Differences may conceivably be attributed to significant couplings between active- and reactive-power injections, withdrawals, and flows that are dealt with by [1] in a disjoint fashion. ■

V. NUMERICAL CASE STUDIES

In this section, we first present results from a numerical case study that focuses on the computational cost of the proposed method. Next, we discuss two applications for the power tracing method developed in Section IV: one focuses on a distribution network with radial topology and the other on a transmission network with meshed topology.

A. Computational Cost for Different Networks

Computationally intensive operations in the proposed method predominantly include algebraic manipulations of network-admittance-like matrices. In Table V, we report the computation times (given the power-flow solution) required to obtain downstream and upstream complex-power disaggregations for the 39-bus New England, 118-bus IEEE, and 2383-bus Polish test systems on a conventional laptop (Intel Core i5 processor at 2.6 GHz with 16 GB 1600 MHz DDR3 memory). The results indicate that downstream power tracing is more computationally expensive compared to upstream power tracing. This is because there are more load buses than generator buses in all three networks. Consequently, algebraic operations in downstream tracing have to be performed with matrices of dimension 29×29 , 64×64 , 2056×2056 for the 39-, 118-, 2383-bus systems, respectively. In contrast, the dimensions of the largest matrices for which we perform algebraic operations in upstream tracing are 10×10 , 54×54 , 327×327 for the 39-, 118-, 2383-bus systems, respectively.

B. Loss Allocation in Distribution Networks

Transmission-loss allocation has long been recognized as a challenging issue due to the nonlinear nature of the power-flow equations [24], [25]. Here, we apply the proposed downstream

TABLE V: Computation times [sec] required to obtain disaggregations in downstream and upstream complex-power tracing for 39-bus New England, 118-bus IEEE, and 2383-bus Polish systems.

	39-Bus	118-Bus	2383-Bus
Downstream	3.01×10^{-4}	1.11×10^{-3}	2.91
Upstream	2.54×10^{-4}	1.05×10^{-3}	1.43

		②	③	④	⑤	Loss	Row Σ
Case (a)	①	0.800	0.500	0.900	1.00	0.138	3.34
	Column Σ	0.800	0.500	0.900	1.00	0.138	3.34
		$-P_{\mathcal{L}}^2$	$-P_{\mathcal{L}}^3$	$-P_{\mathcal{L}}^4$	$-P_{\mathcal{L}}^5$	$\text{Re}\{L\}$	$\sum_{g \in \mathcal{G}} P_{\mathcal{G}}^g$
Case (b)	①	0.800	0.500	0.900	0.500	0.0917	2.79
	Column Σ	0.800	0.500	0.900	0.500	0.0917	2.79
		$-\tilde{P}_{\mathcal{L}}^2$	$-\tilde{P}_{\mathcal{L}}^3$	$-\tilde{P}_{\mathcal{L}}^4$	$-\tilde{P}_{\mathcal{L}}^5$	$\text{Re}\{\tilde{L}\}$	$\sum_{g \in \mathcal{G}} \tilde{P}_{\mathcal{G}}^g$

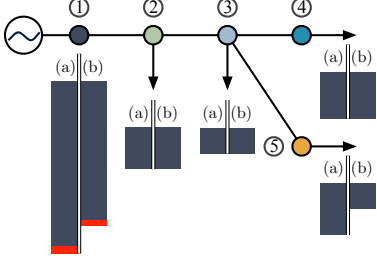


Fig. 7: Downstream active-power tracing in a 5-bus distribution feeder. System loss allocated to feeder head. Case (a): before DG at bus 5; case (b): after DG at bus 5.

TABLE VI: Comparison of upstream tracing results for system in Fig. 8 obtained via the proposed method and the one in [1]. All quantities are in p.u.

Case	(a) [Proposed]		(a) [1]		(b) [Proposed]		(b) [1]	
	①	Loss	①	Loss	①	Loss	①	Loss
②	-0.812	0.0116	-0.811	0.0114	-0.810	0.0103	-0.810	0.0098
③	-0.526	0.0264	-0.523	0.0234	-0.523	0.0226	-0.519	0.0192
④	-0.938	0.0379	-0.949	0.0494	-0.935	0.0352	-0.942	0.0417
⑤	-1.06	0.0621	-1.05	0.0537	-0.524	0.0236	-0.521	0.0209

and upstream power-tracing methods to a representative distribution network, and discuss two ways in which the total feeder loss can be allocated. In the interest of presentation clarity, we focus our attention on only the real part of the complex-valued loss defined in (26).

Consider the 5-bus distribution-system feeder depicted in Fig. 7. Bus 1 represents the feeder head (the secondary of the step-down transformer that connects the feeder to the bulk system) and is modelled as a generator bus. All other nodes are load buses. With regard to the adopted notation, for the system of interest, $\mathcal{G} = \{1\}$ and $\mathcal{L} = \{2, 3, 4, 5\}$. We consider two cases: (a) the active-power injections at load buses are set as $P_{\mathcal{L}}^2 = -0.800$, $P_{\mathcal{L}}^3 = -0.500$, $P_{\mathcal{L}}^4 = -0.900$, and $P_{\mathcal{L}}^5 = -1.00$, all in p.u.; (b) distributed generation (DG) at bus 5 serves some of the local load, and consequently the new net injection at bus 5 is $\tilde{P}_{\mathcal{L}}^5 = -0.500$ p.u. (Injections at other load buses are the same as in case (a).) With this setup, the power-flow solution for case (a) reveals that the feeder head injects $P_{\mathcal{G}}^1 = 3.34$ p.u., with system loss $\text{Re}\{L\} = 0.138$ p.u. In case (b), the feeder head injection is $\tilde{P}_{\mathcal{G}}^1 = 2.79$ p.u., with system loss $\text{Re}\{\tilde{L}\} = 0.0917$ p.u. As expected, the addition of DG reduces the total system loss because less power is required from the feeder head.

1) *Downstream Tracing*: Applying the downstream tracing method and extracting the real part of (27), we obtain the disaggregation of the feeder-head active-power injection into contributions to each load and to the system loss, values from which are reported in the table in Fig. 7. As illustrated by both the table and the one-line diagram in Fig. 7, loss incurred in

	Case (a)			Case (b)		
	①	Loss	Row Σ	①	Loss	Row Σ
②	-0.812	0.0116	-0.800	-0.810	0.0103	-0.800
③	-0.526	0.0264	-0.500	-0.523	0.0226	-0.500
④	-0.938	0.0379	-0.900	-0.935	0.0352	-0.900
⑤	-1.06	0.0621	-1.00	-0.524	0.0236	-0.500
Column Σ	-3.34	0.138	-3.20	-2.79	0.0917	-2.70
	$-P_{\mathcal{G}}^1$	$\text{Re}\{L\}$	$\sum_{\ell \in \mathcal{L}} P_{\mathcal{L}}^{\ell}$	$-\tilde{P}_{\mathcal{G}}^1$	$\text{Re}\{\tilde{L}\}$	$\sum_{\ell \in \mathcal{L}} \tilde{P}_{\mathcal{L}}^{\ell}$

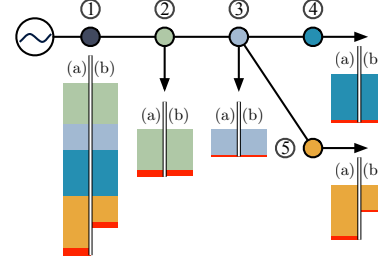


Fig. 8: Upstream active-power tracing in the 5-bus distribution feeder. System loss allocated to each load. Case (a): before DG at bus 5; case (b): after DG at bus 5.

the feeder (marked in red) is allocated to bus 1 (the feeder head). Such an allocation scheme would be useful in operating a vertically integrated power system in which the utility bears the cost of transmission losses. Since this system contains only one generator, there is no ambiguity in allocating generator contributions to loads and loss. Thus, the method in [1] yields the same numerical results.

2) *Upstream Tracing*: The upstream tracing method enables unbundling transmission losses so they can be allocated to each consumer in the distribution network. Extracting the real part of (34), we get the disaggregation of the active-power injection of each load into components that are: i) sourced from the feeder head at bus 1, and ii) allocated to system loss. Particularly, components of each load allocated to the system loss are reported in the table in Fig. 8 for cases (a) and (b). We note that the contribution of a load to loss is affected by two factors: the amount of power demanded by that load and its proximity to the feeder head. As a trend, loads that are located further down the feeder contribute more to loss, see, e.g., contributions from buses 4 and 5 as compared with those from buses 2 and 3 in case (a). On the other hand, in case (b), the load at bus 5 demands less power from the feeder head, and so it contributes less to the system loss. We compare upstream tracing results obtained via the proposed method with the one in [1], and the results are summarized in Table VI. In contrast to Example 4, for this case, we see that the results closely match those obtained from the approach in [1]. This is presumably due to the fact that reactive-power components of loads have little effect on line active-power flows.

C. Bilateral Transaction Allocation

Bilateral transactions are power-trade agreements between suppliers and consumers of electricity. While the financial agreement is settled on a node-to-node basis, the physical paths taken by the transacted power depend on the network topology and parameters. Applying the proposed downstream and upstream tracing methods to the Western Electricity Coordinating

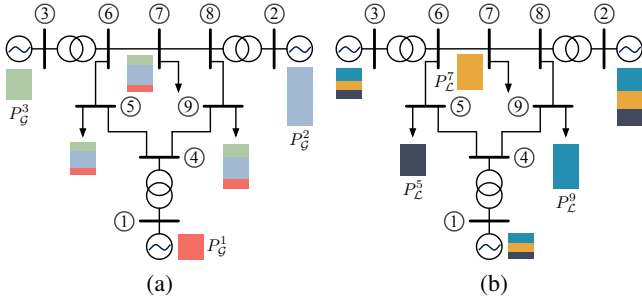


Fig. 9: Tracing active power in the 9-bus network for the base case. (a) Downstream tracing of $P_G^1 = 0.720$ p.u., $P_G^2 = 1.63$ p.u., and $P_G^3 = 0.850$ p.u. (b) Upstream tracing of $P_L^5 = -0.900$ p.u., $P_L^7 = -1.00$ p.u., and $P_L^9 = -1.25$ p.u.

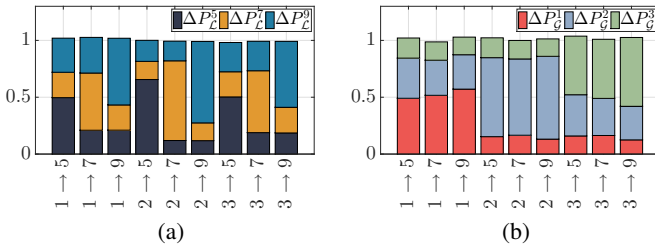


Fig. 10: Contributions of (a) loads and (b) generators for all bilateral transactions of magnitude 1.00 p.u. in the WECC system. ($x \rightarrow y$ represents a transaction where generator at bus x increases output by 1.00 p.u. and load at bus y increases consumption by 1.00 p.u.)

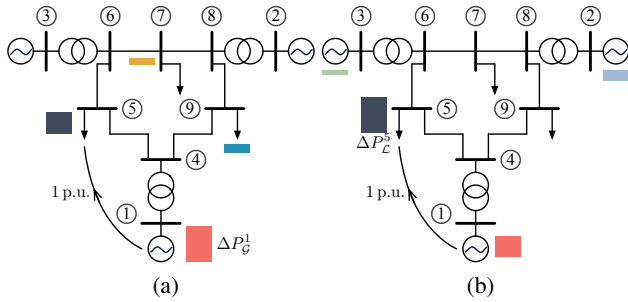


Fig. 11: (a) Downstream and (b) upstream active-power tracing in the WECC system after the 1 \rightarrow 5 bilateral transaction of 1.00 p.u.

Council (WECC) 3-machine 9-bus system, we illustrate how all generators and loads contribute to a bilateral transaction. As a base case, extracting the real part of the generator disaggregation in (27), Fig. 9a shows the downstream active-power tracing from generators to loads. Conversely, upstream active-power tracing is obtained from the real part of (34) and is shown in Fig. 9b.

In Figs. 11a–11b, we plot downstream and upstream disaggregations resulting from all possible bilateral transactions between generator-load pairs of magnitude 1.00 p.u. in the WECC network. Notice that the origin and destination buses assume the largest fraction of the transactions in each case. Closer inspection reveals a slew of nonlinear effects. For instance, the remainder of the buses do not appear to contribute

in proportion to their electrical distances from each transaction consistently. More importantly, these results conclusively demonstrate that *all* nodes in the network contribute to *all* bilateral transactions. While this is intuitive, our approach allows one to numerically quantify contributions of nodal injections and withdrawals to transactions.

VI. CONCLUDING REMARKS AND FUTURE WORK

We developed a circuit-theoretic method to trace complex-power injections from generators to loads (and vice versa). The proposed method leveraged a suite of circuit-theoretic constructs to arrive at the disaggregation of generator (load) complex-power injections into constituent parts, each of which are attributable to loads (generators) and losses. We presented applications of power tracing to loss allocation in distribution networks and bilateral transaction allocation in transmission networks. With numerical case studies, we demonstrated that the proposed method can be implemented with limited computational burden, applies to networks with arbitrary topologies, and reflects the coupling between active- and reactive-power injections.

As part of future work, applications of power tracing to fixed-cost allocation, transmission-services pricing, and validating bilateral transactions for distribution-network markets could be developed. From a theoretical perspective, decoupling assumptions that are common to power systems analysis could be leveraged to not only obtain insights on dependence of tracing coefficients on network attributes but also potentially facilitate computations. Finally, while we provide comparisons of numerical results with those obtained from the proportional sharing method in [1], exhaustive numerical case studies that compare the present approach with a wider body of previous ones could be performed.

REFERENCES

- [1] J. Bialek, "Tracing the flow of electricity," *IEE Proceedings—Generation, Transmission and Distribution*, vol. 143, no. 4, pp. 313–320, July 1996.
- [2] D. Kirschen, R. Allan, and G. Strbac, "Contributions of individual generators to loads and flows," *IEEE Transactions on Power Systems*, vol. 12, no. 1, pp. 52–60, February 1997.
- [3] A. R. Abhyankar, S. A. Soman, and S. A. Khaparde, "Optimization approach to real power tracing: an application to transmission fixed cost allocation," *IEEE Transactions on Power Systems*, vol. 21, no. 3, pp. 1350–1361, August 2006.
- [4] K. M. Jhala, B. Natarajan, A. Pahwa, and H. Wu, "Stability of transactive energy market-based power distribution system under data integrity attack," *IEEE Transactions on Industrial Informatics*, To be published, 2019.
- [5] T. Morstyn, A. Teytelboym, and M. D. Mcculloch, "Bilateral contract networks for peer-to-peer energy trading," *IEEE Transactions on Smart Grid*, vol. 10, no. 2, pp. 2026–2035, March 2019.
- [6] M. T. Devine and P. Cuffe, "Blockchain electricity trading under demurrage," *IEEE Transactions on Smart Grid*, vol. 10, no. 2, pp. 2323–2325, March 2019.
- [7] J. Bialek, "Allocation of transmission supplementary charge to real and reactive loads," *IEEE Transactions on Power Systems*, vol. 13, no. 3, pp. 749–754, August 1998.
- [8] J. W. Bialek and P. A. Kattuman, "Proportional sharing assumption in tracing methodology," *IEE Proceedings—Generation, Transmission and Distribution*, vol. 151, no. 4, pp. 526–532, July 2004.
- [9] F. F. Wu, Y. Ni, and P. Wei, "Power transfer allocation for open access using graph theory-fundamentals and applications in systems without loopflow," *IEEE Transactions on Power Systems*, vol. 15, no. 3, pp. 923–929, August 2000.

- [10] C. Achayuthakan, C. J. Dent, J. W. Bialek, and W. Ongsakul, "Electricity tracing in systems with and without circulating flows: Physical insights and mathematical proofs," *IEEE Transactions on Power Systems*, vol. 25, no. 2, pp. 1078–1087, May 2010.
- [11] D. Kirschen and G. Strbac, "Tracing active and reactive power between generators and loads using real and imaginary currents," *IEEE Transactions on Power Systems*, vol. 14, no. 4, pp. 1312–1319, November 1999.
- [12] A. R. Abhyankar, S. A. Soman, and S. A. Khaparde, "Min-max fairness criteria for transmission fixed cost allocation," *IEEE Transactions on Power Systems*, vol. 22, no. 4, pp. 2094–2104, November 2007.
- [13] M. S. S. Rao, S. A. Soman, P. Chitkara, R. K. Gajbhiye, N. Hemachandra, and B. L. Menezes, "Min-max fair power flow tracing for transmission system usage cost allocation: A large system perspective," *IEEE Transactions on Power Systems*, vol. 25, no. 3, pp. 1457–1468, August 2010.
- [14] J.-H. Teng, "Power flow and loss allocation for deregulated transmission systems," *International Journal of Electrical Power & Energy Systems*, vol. 27, no. 4, pp. 327–333, May 2005.
- [15] W.-M. Lin, T.-S. Zhan, and C.-H. Huang, "A circuit theory based load flow tracing method considering counter-flow contribution," in *Proceedings of the 5th WSEAS International Conference on Instrumentation, Measurement, Circuits and Systems*, 2006, pp. 312–317.
- [16] A. J. Conejo, J. Contreras, D. A. Lima, and A. Padilha-Feltrin, "Zbus transmission network cost allocation," *IEEE Transactions on Power Systems*, vol. 22, no. 1, pp. 342–349, February 2007.
- [17] S. M. Abdelkader, D. J. Morrow, and A. J. Conejo, "Network usage determination using a transformer analogy," *IET Generation, Transmission Distribution*, vol. 8, no. 1, pp. 81–90, January 2014.
- [18] Y. C. Chen and S. V. Dhople, "Power divider," *IEEE Transactions on Power Systems*, vol. 31, no. 6, pp. 5135–5143, November 2016.
- [19] M. Pantos and F. Gubina, "Ex-ante transmission-service pricing based on load-flow patterns," *IEEE Transactions on Power Systems*, vol. 19, no. 2, pp. 796–801, May 2004.
- [20] P. M. Costa and M. A. Matos, "Loss allocation in distribution networks with embedded generation," *IEEE Transactions on Power Systems*, vol. 19, no. 1, pp. 384–389, February 2004.
- [21] A. R. Abhyankar, S. A. Soman, and S. A. Khaparde, "Tractability of bilateral transactions considering multiplicity of solution space in real power tracing," in *IEEE Power India Conference*, 2006, pp. 1–8.
- [22] S. Cvijic and M. D. Ilic, "Part I: A new framework for modeling and tracing of bilateral transactions and the corresponding loop flows in multi-control area power networks," *IEEE Transactions on Power Systems*, vol. 29, no. 6, pp. 2706–2714, November 2014.
- [23] J. A. Taylor, "Financial storage rights," *IEEE Transactions on Power Systems*, vol. 30, no. 2, pp. 997–1005, March 2015.
- [24] A. J. Conejo, F. D. Galiana, and I. Kockar, "Z-bus loss allocation," *IEEE Transactions on Power Systems*, vol. 16, no. 1, pp. 105–110, February 2001.
- [25] Q. Ding and A. Abur, "Transmission loss allocation based on a new quadratic loss expression," *IEEE Transactions on Power Systems*, vol. 21, no. 3, pp. 1227–1233, August 2006.



Sairaj V. Dhople (M'13) received the B.S., M.S., and Ph.D. degrees in electrical engineering from the University of Illinois at Urbana-Champaign, Urbana, IL, USA, in 2007, 2009, and 2012, respectively. He is currently an Associate Professor with the Department of Electrical and Computer Engineering, University of Minnesota, Minneapolis, MN, USA. His research interests include modeling, analysis, and control of power electronics and power systems with a focus on renewable integration. Dr. Dhople received the National Science Foundation CAREER Award in 2015 and the Outstanding Young Engineer Award from the IEEE Power and Energy Society in 2019. He is an Associate Editor for the *IEEE TRANSACTIONS ON ENERGY CONVERSION* and the *IEEE TRANSACTIONS ON POWER SYSTEMS*.



Yu Christine Chen (M'15) received the B.A.Sc. degree in engineering science from the University of Toronto, Toronto, ON, Canada, in 2009, and the M.S. and Ph.D. degrees in electrical engineering from the University of Illinois at Urbana-Champaign, Urbana, IL, USA, in 2011 and 2014, respectively. She is currently an Assistant Professor with the Department of Electrical and Computer Engineering, The University of British Columbia, Vancouver, BC, Canada, where she is affiliated with the Electric Power and Energy Systems Group. Her

research interests include power system analysis, monitoring, and control.